On the behaviour of continuous RC slab strips flexurally strengthened by the NSM technique

G. Dalfré[1], J. Barros[2]

[1]UNILA, Foz do Iguaçu, Brazil; ISISE, University of Minho, Portugal, e-mail: glaucia.dalfre@unila.edu.br, web: http://www.isise.net
[2] ISISE, University of Minho, Campus de Azurém, Portugal, e-mail: barros@civil.uminho.pt, web: http://www.isise.net

ABSTRACT

This work explores the influence of the amount of CFRP in terms of load carrying capacity, ductility and moment redistribution capacity of continuous RC slab strips. In this way, for assessing the predictive performance of a FEM-based computer program, the experimental results obtained by Bonaldo (2008) and Dalfré (2013) were compared with values predicted by this software. Finally, a parametric study is carried out to investigate the influence of the strengthening arrangement and CFRP percentage in terms of load carrying capacity and moment redistribution capacity of continuous RC slab strips flexurally strengthened by the NSM technique.

Keywords Continuous RC slabs, Flexural strengthening, FEM, NSM, Moment Redistribution.

Autor de contacto: Dalfré. Gláucia

1. INTRODUCTION

Extensive research has been conducted on the strengthening of reinforced concrete (RC) structures by using the Externally Bonded Fiber Reinforced Polymer reinforcement technique (FRP-EBR). Since the majority of the tests carried out with NSM strengthened members have been executed with simply supported beams and slabs, there is a lack of experimental and theoretical studies on the effectiveness of the NSM technique, in particular in the moment redistribution capacity of statically indeterminate RC members flexurally strengthened with the NSM technique. Relevant studies on continuous RC members strengthened with NSM technique were conducted by Liu (2005), Liu et al (2006) and Bonaldo (2008). To contribute for a better understanding of the influence of the strengthening arrangement (hogging, sagging or both regions) and percentage of FRP in terms of load carrying capacity, moment redistribution capacity and ductility performance, a parametric study was carried out. This parametric study was performed by executing nonlinear analysis with a computer program based on the Finite Element Method (FEM), whose predictive performance was appraised with the results obtained in experimental programs (Bonaldo 2008 and Dalfré 2013).

2. PARAMETRIC STUDY

The reliability of this study requires the use of a computational tool capable of simulating the relevant aspects of this structural system. For this purpose, the version 4.0 of FEMIX computer program was used. FEMIX 4.0 is a computer code whose purpose is the analysis of structures by the Finite Element Method (FEM). The predictive performance of FEMIX to simulate the behaviour of several type of NSM strengthened RC columns (Barros et al. 2008) and beams (Barros et al. 2011). Also, the experimental programs with statically determinate slab strips carried out by Bonaldo (2008) and Dalfré (2013) were already assessed and a good predictive performance on the simulation of the behaviour of the type of structures in analysis was confirmed. Thus, in this work, a parametric study for the evaluation of the influence of relevant parameters on the load carrying capacity, moment redistribution level and ductility performance of statically indeterminate RC slabs strengthened according to the NSM technique. These parameters are: concrete strength class, percentage of existing longitudinal tensile reinforcement, strengthening configuration, and percentage of CFRP laminates.

2.1. Mechanical properties of the intervenient materials and strengthening arrangements

In the parametric study, the mechanical properties adopted for the concrete strength classes (C12/15, C25/30 or C35/45) were determined following the recommendations of Eurocode 2 (2010) and CEB-FIP Model Code (1993) and are presented in Table 1. The values of the parameters adopted for the constitutive model used to simulate the behaviour of the steel bars are those included in Table 2. The arrangements of the steel reinforcement, dimensions of the cross section, support and load conditions are the same adopted in the experimental/numerical program for the reference slab strip of SL15-H/HS, SL30-H/HS and SL45-H/HS series tested by Bonaldo (2008) and Dalfré (2013). However, distinct strengthening arrangements and bond lengths were applied in the hogging (H) and sagging regions (S), as shown in Figure 1.

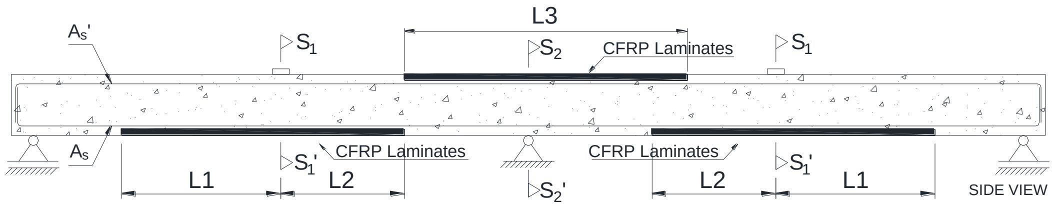

Figure 1: Length of the NSM CFRP laminates for the slab strips.

Table 1: Concrete properties used for the FEM simulations
(Eurocode 2, 2010; CEB-FIP Model Code, 1993; Sena-Cruz, 2004).

Parameters	C12/15	C25/30	C35/45
Compressive strength (N/mm^2)	f_{cm} = 20	f_{cm} = 33	f_{cm} = 43
Initial Young's modulus (N/mm^2)	E_c = 22.85	E_c = 27.21	E_c = 30.82
Poisson's ratio	ν_c =0.00		
Strain at peak compression stress	$\varepsilon_{c1} = 2.80 \times 10^{-3}$	$\varepsilon_{c1} = 2.80 \times 10^{-3}$	$\varepsilon_{c1} = 2.80 \times 10^{-3}$
Tri-linear tension softening [(1)]	f_{ct} = 1.10 N/mm^2 G_f = 0.041 N/mm	f_{ct} = 1.75 N/mm^2 G_f = 0.058 N/mm	f_{ct} = 2.14 N/mm^2 G_f = 0.070 N/mm
	ξ_1= 0.015; α_1= 0.6; ξ_2= 0.2; α_2=0.25		
Parameter defining the initial yield surface	α_0 =0.4		
Parameter defining the mode I fracture energy to the new crack	n=2		
Parameter to define the evolution of the shear retention factor	p_1= 2		
Crack band-width	Square root of the area of Gauss integration point		
Threshold angle	α_{th}= 30°		
Maximum numbers of cracks per integration point	2		

[(1)] $f_{ct} = \sigma^{cr}_{n,1}$; $\xi_1 = \varepsilon^{cr}_{n,2} / \varepsilon^{cr}_{n,u}$; $\alpha_1 = \sigma^{cr}_{n,2} / \sigma^{cr}_{n,1}$; $\xi_2 = \varepsilon^{cr}_{n,3} / \varepsilon^{cr}_{n,u}$; $\alpha_2 = \sigma^{cr}_{n,3} / \sigma^{cr}_{n,1}$ (Sena-Cruz, 2004)

Table 2: Values of the parameters of the steel constitutive model.

Steel bar diameter	$P_1(\varepsilon_{sy}[-];\sigma_{sy}[MPa])$	$P_2(\varepsilon_{sh}[-];\sigma_{sh}[MPa])$	$P_3(\varepsilon_{su}[-];\sigma_{su}[MPa])$	E_s [GPa]
∅ 8mm	(1.90x10^{-3}; 379.16)	(4.42x10^{-2}; 512.19)	(8.85x10^{-2}; 541.66)	200.80
∅ 10mm	(2.32x10^{-3}; 413.20)	(3.07x10^{-2}; 434.75)	(1.31x10^{-1}; 546.25)	178.23
∅ 12mm	(2.09x10^{-3}; 414.35)	(3.05x10^{-2}; 435.63)	(1.02x10^{-1}; 537.98)	198.36

3. RESULTS AND DISCUSSIONS

The slab strips can be classified in three different groups, due to the distinct adopted strengthening arrangements: (a) applied in the hogging region, (b) applied in the sagging regions and (c) applied in both hogging and sagging regions. The notation adopted to identify a slab strip is SLx_y_w_z, where x is the moment redistribution percentage, η (15%, 30% and 45%), y is the concrete strength class (C12/15, C25/30 or C35/45), and w and z indicate the number of NSM CFRP laminates applied in the sagging or hogging regions, respectively. Therefore, SL15_30_4_2 represents a slab with a moment redistribution target of η=15%, made by a concrete of f_{ck}=30 MPa (in cubic specimens), and strengthened with 4 and 2 laminates in the sagging and hogging regions, respectively. In the numerical simulations, the analyses were assumed ended when one of the following two considered failure conditions was attained: (i) when the concrete crushing strain was reached in the sagging region (ε_c^S=3.5‰); (ii) when the effective strain in the CFRP laminates, ε_{fd}, was attained in the sagging or in the hogging region. This ε_{fd} is the maximum tensile strain that can be applied in order to prevent a failure controlled by FRP debonding, also designated by effective failure strain.

According to the ACI 440 (2008), for NSM FRP applications $\varepsilon_{fd} = 0.7\varepsilon_{fu}$, where ε_{fu} is the ultimate strain obtained from uniaxial tensile tests. Figures 2 and 3 summarize the results obtained in the numerical simulations for the three concrete strength classes, respectively. Due to the limited space, only the results concerning to the SL30 Series are represented, but similar behavior was obtained for all the Series. The results obtained allow pointing out the following observations:

1. When the NSM CFRP laminates are applied only in the hogging region, regardless of the concrete strength class, the first plastic hinge (coinciding with the yield initiation of tensile steel bars) occurred at the hogging region, followed by the formation of a plastic hinge in the sagging regions, and the analysis ended due to the concrete crushing occurrence in the sagging regions.

2. For any value of ρ_f^H, regardless the concrete strength class, the increase of ρ_f^S provided an increase of Δ_u and a small decrease of Δ_y, leading to an increase of the deflection amplitude between the formation of the plastic hinges in the hogging and sagging regions (Δ_u - Δ_y), which contributes to better performances of the corresponding strengthening configurations in terms of load-carrying and deflection capacities, as will be observed in next section. In contrast, for any value of ρ_f^S and regardless the concrete strength class, the increase of ρ_f^H provided a decrease of Δ_u and an increase of Δ_y, resulting a decrease of (Δ_u - Δ_y), with a detrimental consequence in terms of load-carrying and deflection capacities.

3. The aforementioned tendencies in terms Δ_y and Δ_u were also observed for the load-carrying capacity (F_y and F_u). In fact, for all the concrete strength classes considered, the increase of F_u with ρ_f^H was much smaller than with the increase of ρ_f^S.

4. The increase of the concrete strength class led to a higher probability of the failure condition to be governed by the attainment of the effective failure strain, ε_{fd}.

The load carrying capacity index (λ) is defined as the ratio between the load carrying capacity of the strengthened $\left(F_{streng}\right)$ and the corresponding reference slab$\left(F_{ref}\right)$, $\lambda = F_{streng} / F_{ref}$, where F is the force at the initiation of the second plastic hinge. The relationships between λ and $\rho_{s,eq}$ in the hogging ($\rho_{s,eq}^H$) and sagging ($\rho_{s,eq}^S$) regions are represented in Figure 2. For the slabs only strengthened in the hogging region, the increase of λ is less than 19%, 22% and 23% for the

SL15, SL30 and SL45 series, which is in agreement to the experimental results presented in Bonaldo (2008) and Dalfré (2013). In the slab strips only strengthened in the sagging region, a maximum increase of 67%, 58% and 39% for the SL15, SL30 and SL45 series was obtained.

As expected, to increase significantly the load carrying capacity of this type of slabs, a flexural strengthening strategy composed by CFRP laminates applied in both hogging and sagging regions should be adopted. According to the results, a maximum increase of 108%, 103% and 97% for the SL15, SL30 and SL45 series was obtained. Additionally, the analysis of the results and the observations of Barros and Kotynia (2008) indicate that the increase of the load carrying capacity with the increase of ρ_f^S and ρ_f^H would be even higher if smaller values of ρ_s^H and ρ_s^S have been used (the values adopted in this parametric study were relatively high for RC slabs).

The moment redistribution index (*MRI*) is defined as the ratio between the η of a strengthened slab, η_{streng}, and the η of its reference slab, η_{ref}, ($MRI = \eta_{streng} / \eta_{ref}$), where η is the moment redistribution percentage at the formation of the second hinge (in the sagging region).

The relationships $MRI - \rho_{s,eq}^S$ and $MRI - \rho_{s,eq}^H$ are shown in Figure 3. In these figures it is also indicated the relationships $MRI - \rho_f^S$ and $MRI - \rho_f^H$. It is observed that the *MRI* depends strongly on the strengthening arrangement. In the slab strips only strengthened in the hogging region η_{streng} is less than η_{ref}. Increasing the percentage of laminates in the sagging region, *MRI* increases, regardless the $\rho_{s,eq}^H$. For slabs only strengthened in the sagging regions, *MRI*>1.0, which means that this type of slabs has higher moment redistribution capacity than its reference slab. However, with the increase of the percentage of laminates in the hogging region the *MRI* decreases. Figure 3 shows a good agreement between the results of the parametric study and the values obtained in the experimental programs described in Bonaldo (2008) and Dalfré (2013).

To avoid a decrease in the moment redistribution capacity, CFRP laminates strips should be applied in both sagging and hogging regions, in appropriate percentages. Figure 4 shows that the moment redistribution index increases with $\rho_{s,eq}^S / \rho_{s,eq}^H$. For $\rho_{s,eq}^S / \rho_{s,eq}^H$>1.09, $\rho_{s,eq}^S / \rho_{s,eq}^H$>1.49 and $\rho_{s,eq}^S / \rho_{s,eq}^H$>2.27 the *MRI* is positive for η equal to 15%, 30% and 45%, respectively.

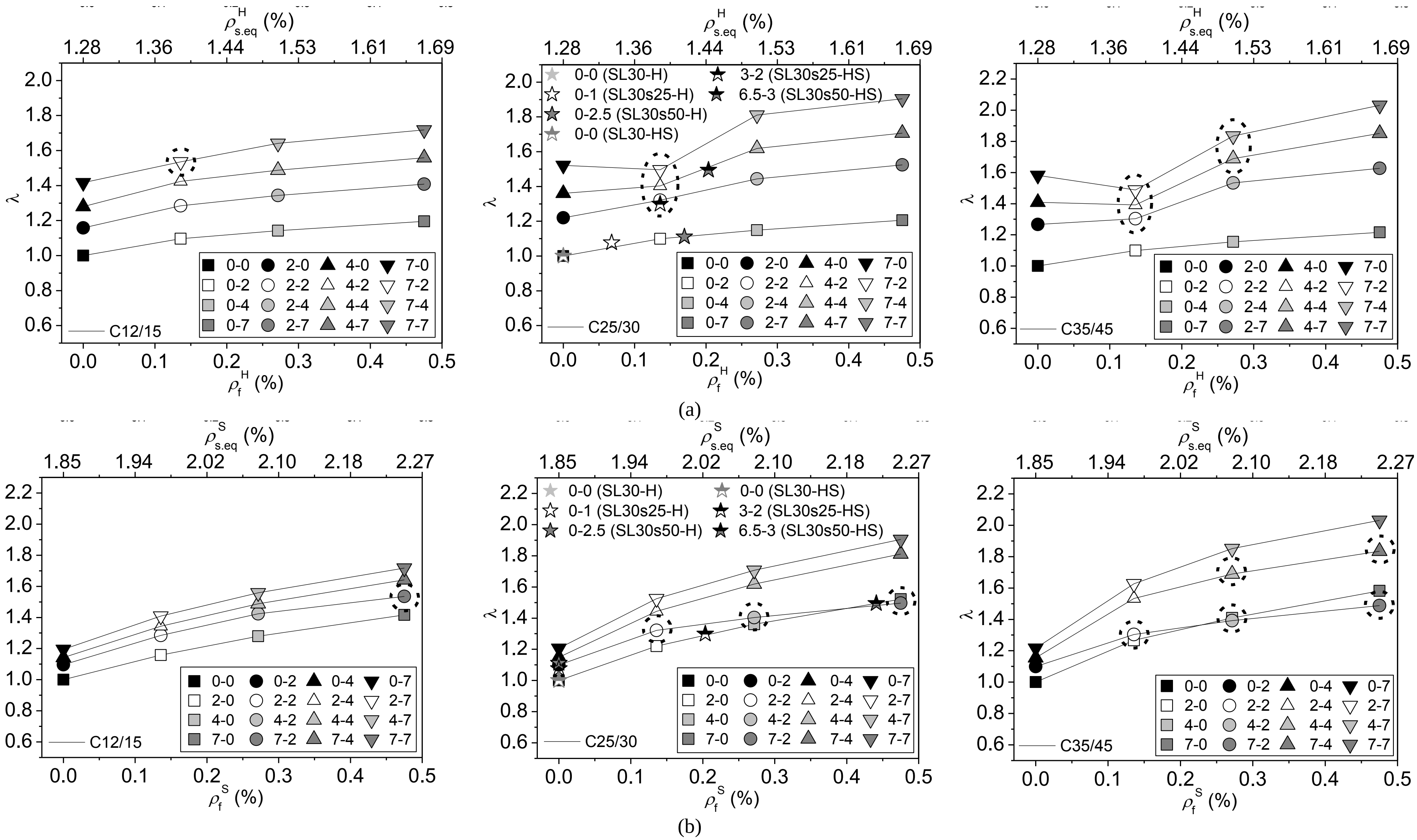

Figure 2: Relationship between the load carrying capacity index, λ, and the CFRP strengthening ratio /equivalent reinforcement ratio in the (a) hogging and (b) sagging regions for the SL30 Series.

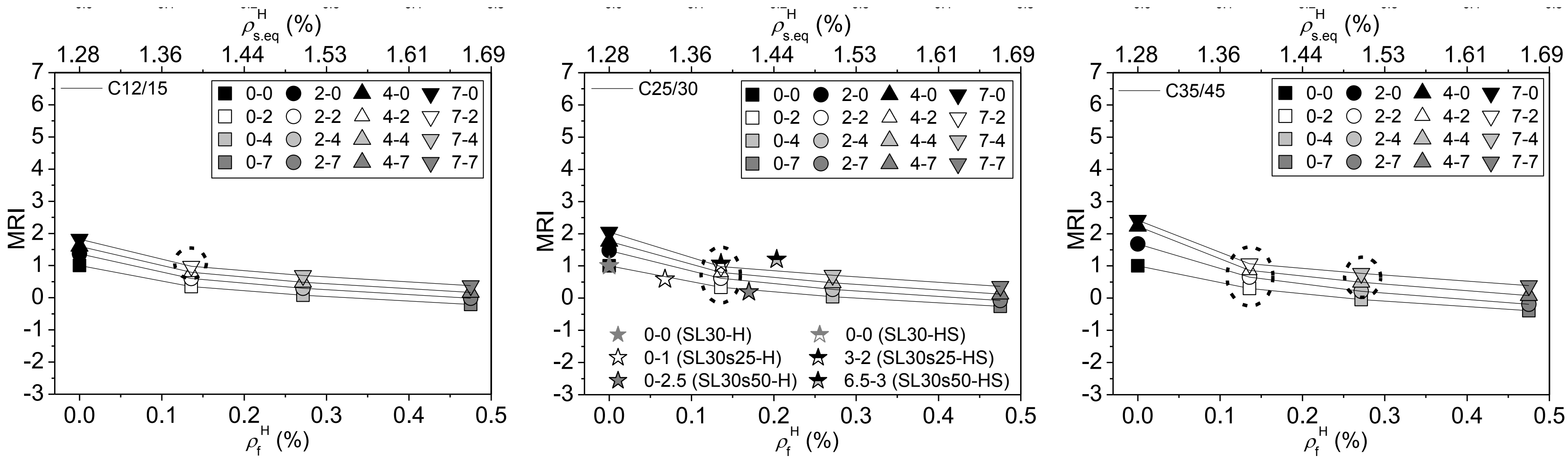

(a)

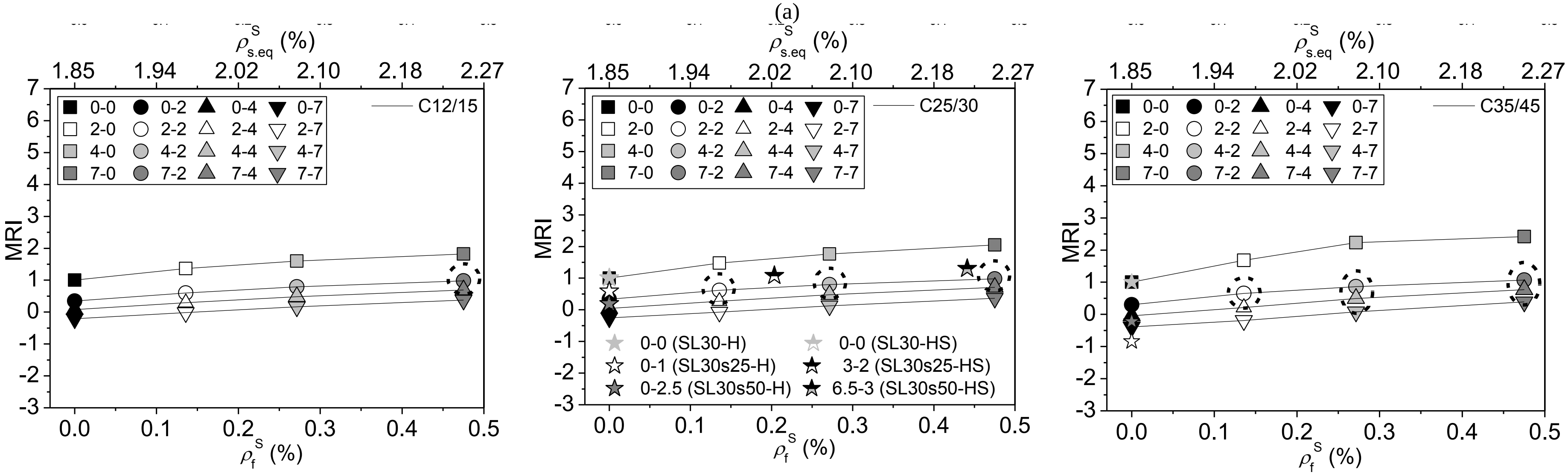

(b)

Figure 3: Relationship between the moment redistribution index, MRI, and the CFRP strengthening ratio/equivalent reinforcement ratio in the (a) hogging and (b) sagging regions for the SL30 Series.

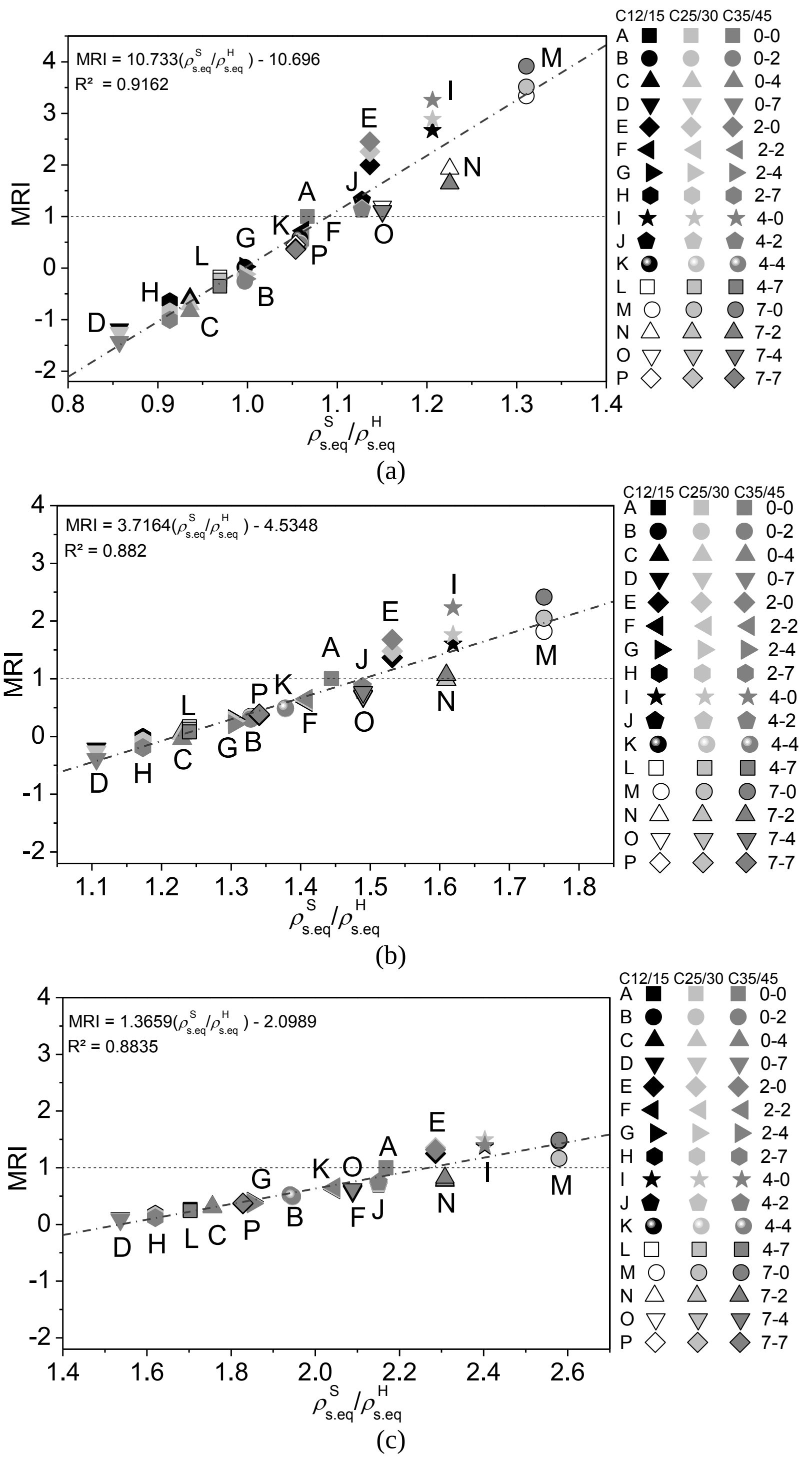

Figure 4: Relationship between the moment redistribution index and $\rho^S_{s,eq}/\rho^H_{s,eq}$ for series: (a) SL15, (b), SL30, and (c) SL45.

4. CONCLUSIONS

To evaluate the influence of the concrete strength class, the percentage of existing longitudinal tensile reinforcement and the percentage of CFRP on the strengthening effectiveness, moment redistribution capacity and ductility performance, a parametric study was carried out by executing material nonlinear analysis with a FEM-based computer program, which predictive performance was calibrated using the results of the experimental programs performed by Bonaldo (2008) and Dalfré (2013). From the obtained results it can be pointed out the following main observations:

(i) The overall behaviour of the strengthened slab strips is not significantly affected by the concrete strength class, as long as structural concrete strength classes, according the Model Code classification, are used;

(ii) The load carrying and the moment redistribution capacities strongly depend on the flexural strengthening arrangement;

(iii) The load carrying capacity of the strengthened slabs increases with $\rho_{s,eq}^{S}$ and $\rho_{s,eq}^{H}$, but the increase is much more pronounced with $\rho_{s,eq}^{S}$, specially up to the formation of the plastic hinge in the hogging region ($\rho_{s,eq} = A_{sl} / bd_s + (A_f E_f / E_s) / (bd_f)$ is the equivalent reinforcement ratio);

(vi) The moment redistribution decreases with the increase of $\rho_{s,eq}^{H}$, and increases with $\rho_{s,eq}^{S}$;

(v) The moment redistribution increases with $\rho_{s,eq}^{S} / \rho_{s,eq}^{H}$ and positive values (which means that the moment redistribution of the strengthened slab is higher than its corresponding reference slab) are positive when $\rho_{s,eq}^{S} / \rho_{s,eq}^{H}$ >1.09, $\rho_{s,eq}^{S} / \rho_{s,eq}^{H}$ >1.49 and $\rho_{s,eq}^{S} / \rho_{s,eq}^{H}$ >2.27 for η equal to 15%, 30% and 45%, respectively. Additionally, when considering all the series analysed in this work, a good fit for a linear model was obtained for $\eta - \rho_{s,eq}^{S} / \rho_{s,eq}^{H}$. Thus, the moment redistribution percentage can be estimated by using the parameter $\rho_{s,eq}^{S} / \rho_{s,eq}^{H}$;

(vi) A flexural strengthening strategy composed of CFRP laminates applied in both hogging and sagging regions has a deflection ductility performance similar to its corresponding RC slab.
In conclusion, the obtained results evidence that the use of efficient strengthening strategies can provide adequate level of ductility and moment redistribution in statically indeterminate structures, with a considerable increase in the load carrying capacity.

5. ACKNOWLEDGMENTS

The first author acknowledges the financial support of FCT (PhD Grant number SFRH/BD/69818/2010) and the National Council for Scientific and Technological Development (CNPq) – Brazil (GDE 200953/2007-9).

6. REFERENCES

ACI Committee 440 (2008), *Guide for the design and construction of externally bonded FRP systems for strengthening concrete structures*, ACI440.2R-08, Reported by ACI Committee 440, American Concrete Institute, Farmington Hills, Mich, 80 pp.

Barros J.A.O, Varma, R.K., Sena-Cruz, J.M., Azevedo, A.F.M. (2008), *Near surface mounted CFRP strips for the flexural strengthening of RC columns - experimental and numerical research*, Engineering Structures Journal, 30(12), pp. 3412-3425.

Barros, J.A.O., Kotynia, R. (2008), *Possibilities and challenges of NSM for the flexural strengthening of RC structures*, Fourth International Conference on FRP Composites in Civil Engineering (CICE2008), Zurich, Switzerland, 22-24 July.

Barros J.A.O, Costa, I.G., Ventura-Gouveia, A. (2011), *CFRP flexural and shear strengthening technique for RC beams: experimental and numerical research*, Advances in Structural Engineering Journal, 14(3), pp. 551-573.

Bonaldo E. (2008), C*omposite materials and discrete steel fibres for the strengthening of thin concrete structures*, PhD Thesis, University of Minho, Guimarães, Portugal.

CEB-FIP Model Code 1990 (1993), *Design Code,* Thomas Telford, Lausanne, Switzerland.

Dalfré G.M. (2013), *Flexural and shear strengthening of RC elements,* PhD Thesis, University of Minho, Portugal, in press.

EN 1992-1-1 (2010), *Eurocode 2: Design of Concrete Structures-Part 1-1: General Rules and Rules for Buildings*, CEN, Brussels.

Liu I.S.T. (2005), *Intermediate crack debonding of plated reinforced concrete beams*, PhD Thesis, School of Civil and Environmental Engineering, The University of Adelaide, Adelaide, Australia.

Liu I.S.T., Oehlers D.J., Seracino R. (2006), *Tests on the ductility of reinforced concrete beams retrofitted with FRP and steel near-surface mounted plates*, Journal of Composites for Construction, 10(2), pp. 106-114.

Sena-Cruz J. M. (2004), *Strengthening of concrete structures with near-surface mounted CFRP laminate strips*, PhD Thesis, Department of Civil Engineering, University of Minho, Portugal.